

# Development of Carburizing Steel for Innovation in Parts Manufacturing Process<sup>†</sup>

IMANAMI Yuta\*<sup>1</sup> TOMITA Kunikazu\*<sup>2</sup> NISHIMURA Kimihiro\*<sup>3</sup>

## Abstract:

In order to develop a new carburizing steel that realizes an intermediate heat treatment-free process (omission of annealing before cold forging and normalizing before carburizing) in the manufacture of carburized parts, the cold forgeability of the as-rolled steel and suppression of abnormal grain growth of austenite ( $\gamma$ ) during carburizing were studied. It was shown that optimization of the balance of Si, Mn and Cr addition, suppression of dynamic strain aging by fixing N, and an increase of the ferrite fraction by low temperature controlled rolling are effective for reduction of deformation resistance, and Nb precipitation control is necessary for suppression of abnormal grain growth of  $\gamma$ . The new carburizing steel, which was developed by integrating these technologies, makes it possible to eliminate both annealing before cold forging process and normalizing before carburizing, as it displays excellent cold forgeability in the as-rolled condition and suppression of abnormal grain growth of  $\gamma$  during carburizing. Thus, the developed steel is an important innovation in the parts manufacturing process. The name of developed steel is JECF<sup>TM</sup>.

## 1. Introduction

Machine parts such as automotive gears have complicated shapes, and many are manufactured by hot or cold forging using steel for carburizing as the starting material, followed by carburizing heat treatment. Cold forging enables near net shape forming because it has the advantage of excellent dimensional accuracy.

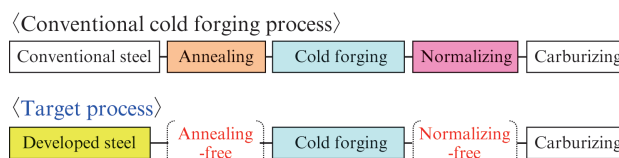


Fig. 1 Conventional process and target process

Therefore cold forging makes it possible to improve yield and productivity by reducing the cutting amount after forging. The general manufacturing process of cold forging parts is shown in **Figure 1**. In cold forging, annealing is generally used to reduce deformation resistance, and normalizing before carburizing is also widely used to suppress abnormal grain growth of  $\gamma$  during carburizing. However, due to intensified parts price competition in recent years, development of steel with high cost competitiveness, for example, by omitting annealing and normalizing, has become important. In order to develop a SCM420 substitute steel which makes it possible to eliminate intermediate heat treatments in the cold forging process, cold forgeability and suppression of abnormal grain growth of  $\gamma$  were investigated.

## 2. Material Development for Omission of Heat Treatment

### 2.1 Improvement of Cold Forgeability

Deformation resistance and the forming limit are considered to be important factors in cold forgeability. In general, reduction of static strength such as hard-

<sup>†</sup> Originally published in *JFE GIHO* No. 39 (Feb. 2017), p. 37–42



\*<sup>1</sup> Senior Researcher Deputy Manager,  
Steel Bar & Wire Rod Research Dept.,  
Steel Res. Lab.,  
JFE Steel



\*<sup>2</sup> Dr. Eng.,  
Senior Researcher General Manager,  
Steel Bar & Wire Rod Research Dept.,  
Steel Res. Lab.,  
JFE Steel



\*<sup>3</sup> General Manager,  
Steel Bar & Wire Rod Research Dept.,  
Steel Res. Lab.,  
JFE Steel

ness and tensile strength is effective for reducing deformation resistance<sup>1)</sup>. However, because cold forging is characterized by a large strain rate, which causes a temperature increase due to plastic deformation, it is also necessary to consider dynamic work hardening<sup>2, 3)</sup>.

Steel for carburizing is a kind of steel having relatively high hardenability as represented by SCM 420 of the JIS standard, and it exhibits a ferrite and pearlite microstructure including bainite depending on the cooling rate after rolling. Among these microstructures, bainite has the highest hardness and ferrite has the lowest hardness. Therefore, in order to reduce the deformation resistance, it is necessary to suppress the formation of bainite so as to form a microstructure composed of ferrite and pearlite, and as much as possible it is ideal to raise the ferrite fraction. The effect of hot rolling conditions on the as-rolled microstructure was investigated with the aim of obtaining this ideal microstructure.

Si, Mn and Cr in steel have a large influence on hardness after hot rolling through their effects on the solid solution strengthening of ferrite<sup>4)</sup> and the lamellar spacing of pearlite<sup>5)</sup>. Since these elements also strongly influence hardenability, their influences on hardness after hot rolling and hardenability were investigated in order to achieve both low hardness on the same level as annealed SCM420 in the as-rolled condition and hardenability comparable to that of SCM420.

As a result of the temperature increase caused by plastic deformation during cold forging, dynamic strain aging due to solid solution N is considered to increase work hardening, and this influences deformation resistance<sup>6)</sup>. Therefore, suppression of dynamic strain aging by fixing solid solution N was investigated.

Regarding the forming limit, after hot rolling, the developed steel exhibits a ferrite and pearlite microstructure, as described above. In contrast, annealed SCM420 has a microstructure consisting of spheroidized cementite dispersed in the ferrite matrix. The effect of this difference in the microstructure on the forming limit was investigated.

## 2.2 Suppression of Abnormal Grain Growth

If austenite causes abnormal grain growth (secondary recrystallization) during carburizing, fatigue property is pronouncedly deteriorated as compared with steels without abnormal grain growth<sup>7)</sup>. In addition, when cold forging is performed before carburizing, the occurrence of abnormal grain growth is accelerated by the influence of strain introduced during forging<sup>8)</sup>. For this reason, additional normalizing before carburizing has been unavoidable with steels such as SCM420 in order to suppress abnormal grain growth. In general, grain boundary pinning by fine dispersion of precipi-

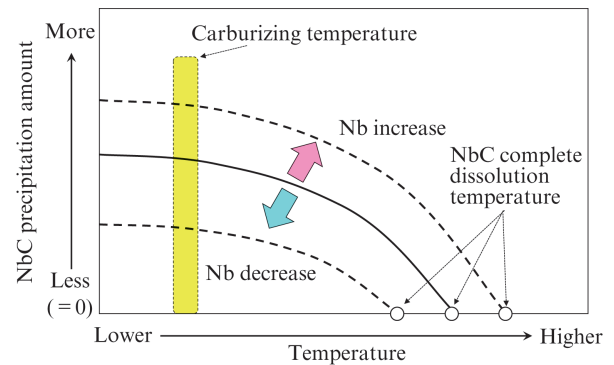


Fig. 2 NbC precipitation curve

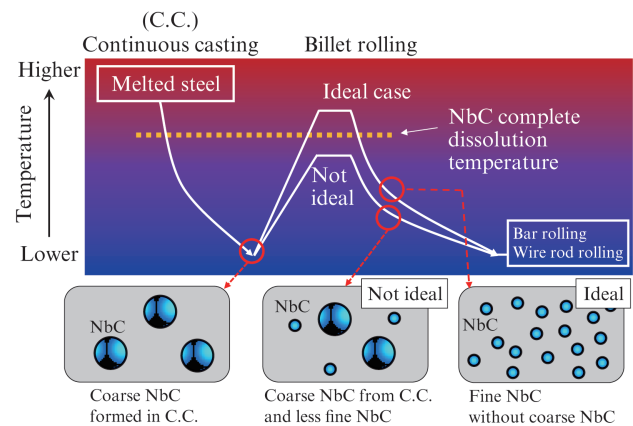


Fig. 3 Control of NbC in manufacturing process

tates is effective to suppress abnormal grain growth. Carbonitride former elements such as Nb, Ti and V are mainly used to form such fine precipitates<sup>9-23)</sup>. However, Ti has the risks of decreasing suppression ability of abnormal grain growth by forming coarse TiN and increasing fatigue initiation sites<sup>24)</sup>. Moreover, reduced machinability due to the formation of Ti sulfides and reduction of Mn sulfides is also a concern. With V, it is difficult to secure the precipitates necessary to exert a sufficient pinning force because dissolution of the precipitates proceeds in the carburizing temperature region (1 173 K–1 223 K). Therefore, steel containing only added Nb was used in this development, and the optimal precipitation control method for Nb was studied.

Both maximizing the amount of precipitates and reducing the size of the precipitates are important for improving the grain boundary pinning force<sup>25)</sup>. In the thermodynamic equilibrium state, the relationship between temperature and the amount of precipitation can generally be calculated from the solubility product of the precipitates. For example, **Figure 2** is a schematic representation of the relationship between temperature and the precipitation amount in the case of NbC (hereinafter, NbC precipitation curve). As the temperature increases, the precipitation amount of NbC decreases. On the other hand, as the amount of Nb addition

increases, the NbC precipitation amount also has a tendency to increase. Here, the intersection of the NbC precipitation curve and the x-axis shows the complete dissolution temperature of NbC. This temperature becomes higher as the amount of Nb addition increases. Assuming an actual hot rolling process, **Figure 3** shows an ideal precipitation control method constructed based on the NbC precipitation curve. Coarse Nb precipitates exist in blooms obtained by continuous casting followed by air cooling. If these coarse Nb precipitates remain until carburizing, precipitation of fine NbC decreases, and a sufficient pinning force cannot be obtained. To prevent this problem, heating to above the complete dissolution temperature of NbC by increasing the hot rolling heating temperature is effective for dissolving coarse Nb precipitates. Although increasing the amount of Nb is effective for increasing fine NbC precipitates and thereby increasing the pinning force, it is necessary to control the upper limit of Nb addition within the range where complete dissolution is possible in the hot rolling process.

### 3. Experimental Procedure

#### 3.1 Cold Forgeability

**Table 1** shows the chemical compositions of the tested steels. To investigate the influence of the hot rolling temperature on the as-rolled microstructure, with Steel A, hot working was done with a Thermecmator (manufactured by Fuji Electronic Industrial Co., Ltd.), followed by etching with 3% nital and observation by optical microscopy.

To investigate the effects of the Si, Mn and Cr contents on hardness after hot rolling, Steels B to G with different Si, Mn and Cr contents were melted, heated to 1473 K, and then air-cooled after hot rolling, and Vickers hardness (HV) was measured.

To investigate the effect of solute N on dynamic strain aging, N solid solution steel (Steel H) and N fixed steel (Steel I) were melted. In the N fixed steel, the N content of the steel was reduced, and a nitride forming element was also added. These samples were

air-cooled after hot rolling, and tensile tests were carried out at the strain rate of  $1s^{-1}$  in an atmosphere with a temperature of 473 K to simulate the temperature increase due to plastic deformation during cold forging.

After alloy design, the cold forgeability of the developed steel manufactured with actual equipment (hereinafter, developed steel) was evaluated by the deformation resistance and forming limit of the as-rolled steel. Measurement of deformation resistance was conformed to the cold upsetting test method established by the Cold Forging Subcommittee of the Japan Society for Technology of Plasticity<sup>26)</sup>. That is, deformation resistance was calculated from the compression load at the upsetting ratio of 60% by using a cylindrical test piece with dimensions of  $\phi 15 \times 22.5$  mm. The forming limit was measured with a cylindrical test piece having dimensions of  $\phi 15 \times 22.5$  mm with a longitudinal V groove (R0.15, depth 0.8, opening angle  $30^\circ$ ). Sequential upsettings were repeated until a crack size of 0.5 mm was observed. As a comparison steel, SCM420 was prepared by spheroidizing annealing, and the deformation resistance and forming limit were compared. After these sequential upsettings, the test pieces were observed with a scanning electron microscope (SEM) to investigate the void generation behavior in the vicinity of the crack.

#### 3.2 Suppression of Abnormal Grain Growth

A number of reports have been published on the solubility product of NbC<sup>27-36)</sup>, but different values have been reported by various researchers. Therefore, the optimal NbC solubility product in Nb-added carburizing steel was examined. Steels J to L with different Nb contents were melted and subjected to heat treatments simulating billet rolling and steel bar rolling, assuming the actual rolling processes. The samples were then cold rolled at the total reduction of 50%, quasi-carburized at  $930^\circ C$  for 3 h, and quenched in oil. Precipitates were observed by transmission electron microscope (TEM), and the precipitation amount was measured by the electrolytic extraction residue method.

In order to evaluate ability of the developed steel to

Table 1 Chemical compositions of steels

| (Mass%) |     |        |        |        |     |        |      |
|---------|-----|--------|--------|--------|-----|--------|------|
| Steel   | C   | Si     | Mn     | Cr     | Mo  | Nb     | N    |
| SCM420  | 0.2 | 0.2    | 0.8    | 1.1    | 0.2 | –      | 0.01 |
| A       | 0.2 | 0.2    | 0.8    | 1.1    | –   | –      | 0.01 |
| B-G     | 0.2 | Varies | Varies | Varies | –   | –      | 0.01 |
| H       | 0.2 | 0.2    | 0.8    | 1.1    | –   | –      | 0.01 |
| I       | 0.2 | 0.2    | 0.8    | 1.1    | –   | –      | Tr.  |
| J-L     | 0.2 | 0.2    | 0.8    | 1.1    | –   | Varies | Tr.  |

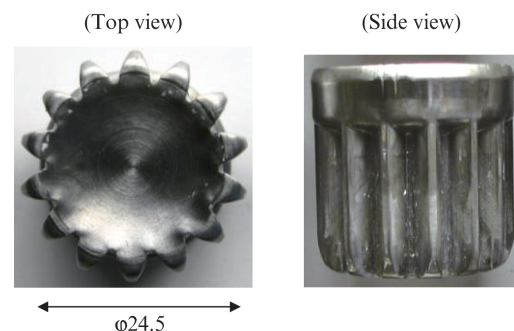


Fig. 4 Gear test piece obtained by cold forging

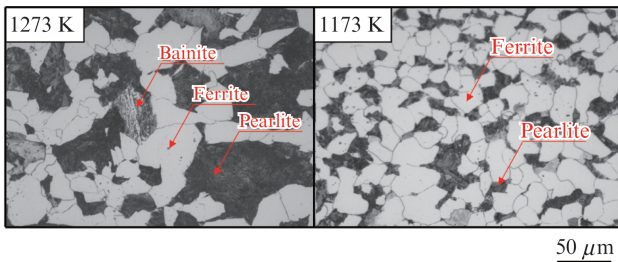


Fig. 5 Optical micrographs of Steel A after hot working

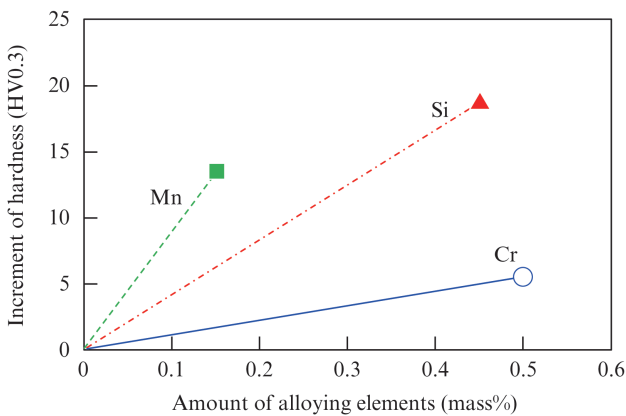


Fig. 6 Relationship between amount of Si, Mn and Cr and hardness

suppress abnormal grain growth of  $\gamma$ , the as-rolled material was cold forged to a gear shape (Figure 4), and quasi-carburizing was performed by quenching after holding at 1 203 K for 3 h. Normalizing was not performed. The prior austenite was observed by optical microscopy after etching the gear cross section with an aqueous solution of picric acid with added benzenesulfonic acid. The SCM420 comparison steel was also evaluated in the same manner.

#### 4. Experimental Results and Discussion

Figure 5 shows the microstructure of Steel A after the Thermecmastor hot working test. Partial formation of bainite could be observed in the steel hot worked at 1 273 K, but the steel hot worked at 1 173 K exhibited a ferrite and pearlite microstructure. Although the crystal grain size was refined in Steel A, which was hot worked at 1 173 K, the hardness of this material decreased about  $\Delta$ HV40 compared to the sample hot worked at 1 273 K. From this, in the range of the present study, it is thought that the hardness decrease resulting from the suppression of bainite formation and the increase in the ferrite fraction is more dominant than the hardness increase due to grain refinement.

Figure 6 shows the relationship between the hardness increase after hot rolling and the amounts of Si, Mn and Cr. Addition of Si and Mn causes a large

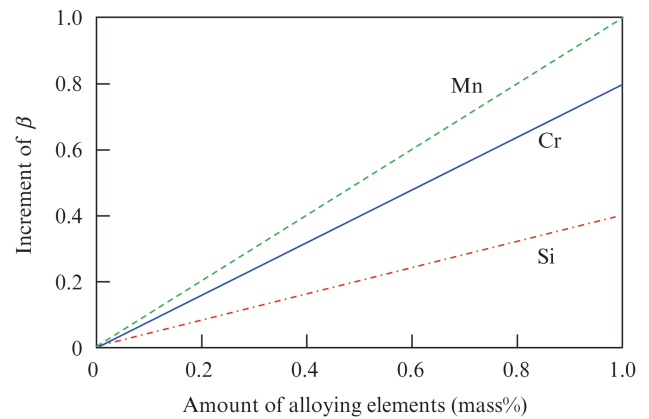


Fig. 7 Relationship between amount of Si, Mn and Cr and hardenability

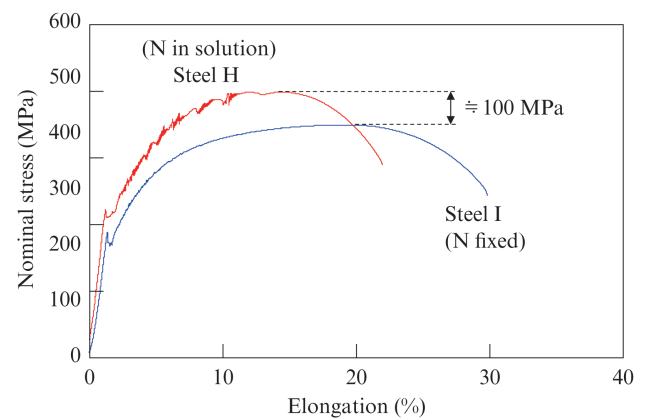


Fig. 8 Stress-strain curves of Steels H and I at 473K

increase in hardness compared to addition of Cr. In order to ensure hardness after carburizing, hardenability is required in carburizing steel. Figure 7 shows the effects of the amount of Si, Mn and Cr addition on the hardenability index  $\beta$  value (Mn equivalent value) obtained by the hardenability prediction equation<sup>37)</sup> proposed by Ueno et al. Mn has a somewhat stronger effect, but Cr also has a similar effect, while the effect of Si is clearly small.

From the above study results, an alloy design in which Si and Mn are reduced and Cr is increased is considered appropriate for achieving both low hardness and sufficient hardenability. Reduction of Si is also preferable from the viewpoint of improving fatigue property by contributing to suppression of grain boundary oxidation of the surface layer after carburizing<sup>38)</sup>. Increasing Cr can be expected to improve pitting fatigue strength through improvement of tempering softening resistance<sup>39)</sup>.

Figure 8 shows the results of the 473 K tensile test of the N solid solution steel (Steel H) and the N fixed steel (Steel I). Remarkable work hardening with serrations, which are a feature of the dynamic strain aging phenomenon, was observed in the N solid solution steel. On the other hand, in the N fixed steel, flow

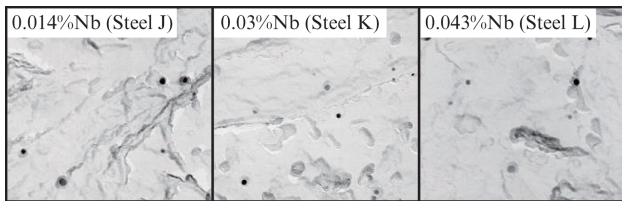


Fig. 9 TEM images of precipitates after quasi-carburizing

Table 2 Values of Nb measured by extraction residue test method and calculated by Irvine solubility product

| Steels       | Nb amount as Nb precipitates |                  |
|--------------|------------------------------|------------------|
|              | Measured value               | Calculated value |
| J (0.014%Nb) | 0.013%                       | 0.012%           |
| K (0.03%Nb)  | 0.028%                       | 0.028%           |
| L (0.043%Nb) | 0.039%                       | 0.041%           |

stress was reduced by approximately 100 MPa by suppression of dynamic strain aging. From this result, suppressing the dynamic strain aging due to the temperature increase caused by plastic deformation during cold forging was shown to be effective for reducing deformation resistance.

#### 4.2 NbC Solubility Product

Figure 9 shows the results of TEM observation of the precipitates of Steels J to L with different Nb contents after quasi-carburizing. All of the precipitates were identified as Nb (C, N) by EDX (Energy Dispersive X-ray) analysis. The size of the Nb (C, N) precipitates was 20 nm or less regardless of the amount of Nb added.

Table 2 shows the amount of precipitated Nb measured by the extraction residue method and the amount at 1 203 K as calculated by the solubility product reported by Irvine<sup>36)</sup>. The experimental and calculated values were in good agreement regardless of the amount of Nb added. From the above results, it was judged that the NbC precipitation curve calculated from the solubility product according to Irvine can be used for precipitation control of Nb in the range of Nb addition in this experiment, and this was used in the alloy design of the developed steel.

### 5. Evaluation of Properties of Developed Steel

Alloy design was performed based on the results described above, and the properties of the as-rolled developed steel produced with actual equipment were evaluated by comparison with the spheroidizing annealed SCM420.

Figure 10 and Figure 11 show the results of the evaluation of deformation resistance and the forming limit

Table 3 Chemical composition of developed steel. (MASS%)

| Steel     | C   | Si         | Mn         | Cr         | Mo  | N                 | Others |
|-----------|-----|------------|------------|------------|-----|-------------------|--------|
| SCM420    | 0.2 | 0.2        | 0.8        | 1.1        | 0.2 | 0.01              | –      |
| Developed | 0.2 | $\leq 0.1$ | $\leq 0.7$ | $\geq 1.3$ | –   | Reduced and fixed | Nb     |

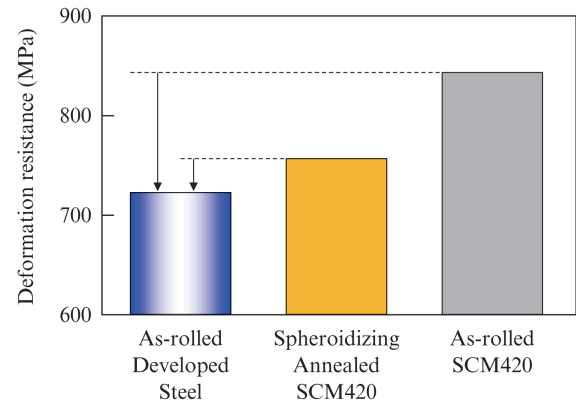


Fig. 10 Deformation resistance of developed steel

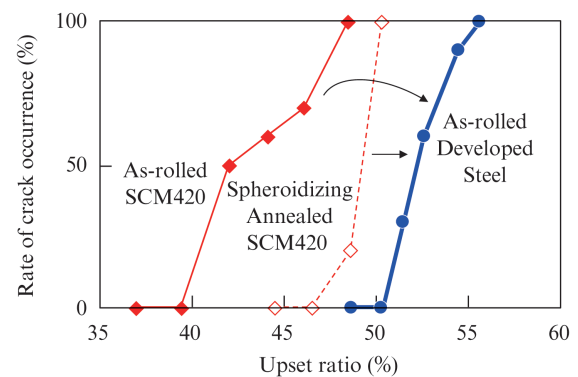


Fig. 11 Forming limit of developed steel

(limit upset-ability), respectively. The as-rolled developed steel showed lower deformation resistance than the spheroidizing annealed SCM420, and the forming limit was also greatly improved.

The reduction of deformation resistance in the developed steel is due to the synergistic effects of the optimized balance of Si, Mn and Cr, suppression of dynamic strain aging by fixing N, and the increase in the ferrite fraction by low temperature controlled rolling. Figure 12 shows the results of SEM observation of the vicinity of the V groove of the test pieces after upsetting. In the annealed SCM420 with spheroidized cementite (Figure 12 (b), (d)), a pronouncedly large number of microvoids (shown by the arrows in the figure) occurred at the cementite-ferrite interfaces. In comparison with this, void formation was suppressed in the developed steel (Figure 12 (a), (c)) with lamellar cementite. This difference was presumably a factor in the improvement of the forming limit of the developed steel. Since the morphology of cementite influences the

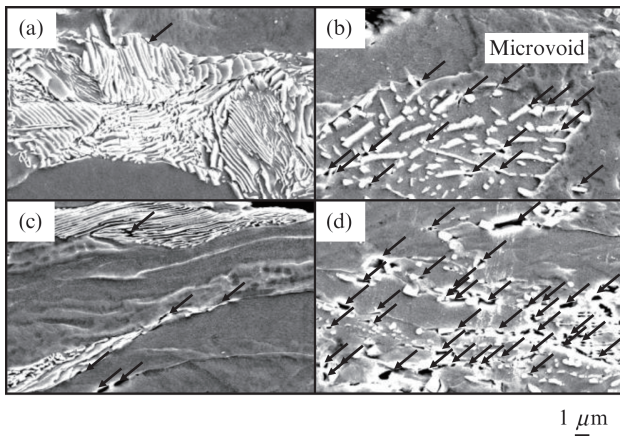
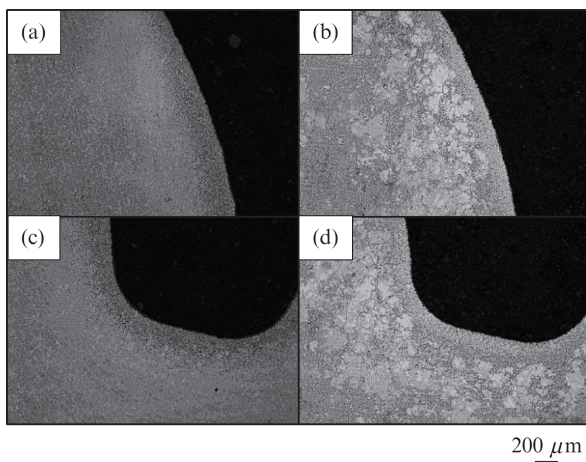


Fig. 12 Void formation behavior in forming limit test



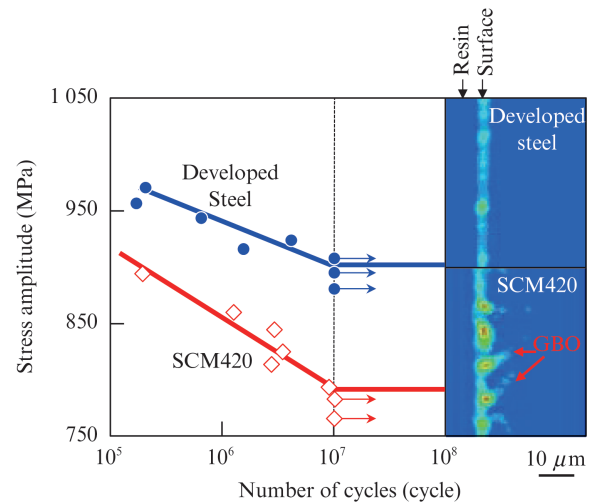
(a) Developed steel at 40% upset  
 (b) Annealed SCM420 at 40% upset  
 (c) Developed steel at 50% upset  
 (d) Annealed SCM420 at 50% upset

Fig. 13 Prior austenite after quasi-carburizing

microvoid formation mechanism<sup>40)</sup>, it is thought that the difference in the microvoid formation behavior in the as-rolled developed steel and the spheroidizing annealed SCM420 was caused by the difference in the cementite morphologies of the two steels.

### 5.2 Suppression of Abnormal Grain Growth

Figure 13 shows the results of observation of prior austenite grains after quasi-carburizing without normalizing for cold forged gears of the developed steel and SCM420. In SCM420, remarkable abnormal grain growth of  $\gamma$  exceeding the grain diameter of  $100\ \mu\text{m}$  occurred at the tooth root and the vicinity of pitch circle, but in the developed steel,  $\gamma$  grains remained fine and abnormal grain growth was not observed. Thus, the developed steel enables suppression of abnormal grain growth of  $\gamma$  without normalizing before carburizing.



(a) Developed steel at pitch circle (b) SCM420 at pitch circle  
 (c) Developed steel at root (d) SCM420 at root  
 Fig. 14 Rotating bending fatigue property after carburizing

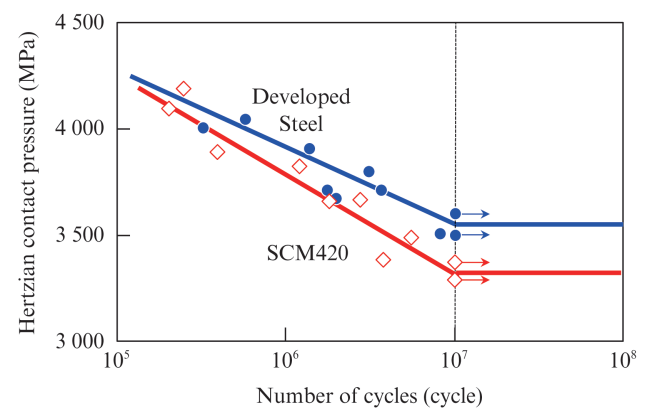


Fig. 15 Contact fatigue property after carburizing

### 5.3 Mechanical Properties after Carburizing

As mechanical properties after carburizing, the results of the rotating bending fatigue test and the roller pitting fatigue test are shown in Figure 14 and Figure 15, respectively.

Rotating bending fatigue strength is an indicator of resistance to breakage of gears. The rotating bending fatigue strength of the developed steel is excellent in comparison with that of SCM420, showing that the developed steel has superior performance in preventing breakage of gears. From the Si mapping by EPMA of the carburized surface layer shown in the same figure, grain boundary oxidation (GBO) was suppressed in the developed steel. The improvement in the rotating bending fatigue strength of the developed steel is considered to be due to the synergistic effects of suppression of grain boundary oxidation and suppression of abnormal grain growth of  $\gamma$ .

Roller pitting fatigue strength is an indicator of resistance to surface fatigue (pitting) of gears. The developed steel showed surface fatigue strength on the

same level as SCM420. The developed steel exhibited the same surface fatigue strength as SCM 420, indicating that the normalizing can be omitted. Surface fatigue properties are reported to show a correlation with tempering softening resistance<sup>39)</sup>. The tempering softening resistance of the developed steel was comparable to that of SCM420 because the Cr content was increased instead of reducing Mo, and as a result, the developed steel is considered to display surface fatigue properties on the same level as SCM420.

From the above fatigue test results, it can be concluded that the mechanical properties of the developed steel after carburizing are equal to or higher than those of SCM420.

## Conclusion

With the developed carburizing steel, it is possible to omit both annealing and normalizing in the cold forging process because this steel possesses excellent cold forgeability in the as-rolled condition and has an suppression ability of abnormal grain growth of  $\gamma$ . Thus, this new steel realizes a significant innovation in the parts manufacturing process. As shown below, since the effects obtained using developed steel are various, it is expected to contribute to a wide range of society. The name of developed steel is JECF<sup>TM</sup>.

[Expected effects of developed steel]

- (1) Omission of annealing before cold forging (drawing)
- (2) Omission of normalizing before carburizing (also possible with hot forged parts)
- (3) Improved tool life due to decrease of deformation resistance
- (4) Expansion of range of shapes that can be cold forged by decrease of deformation resistance and increase of forming limit
- (5) Cost reduction by cold forging of parts conventionally manufactured by hot forging

## References

- 1) Kudo, H.; Sato, K.; Aoi, K.; Sawano, I. *Journal of the Japan Society for Plasticity*. 1968, vol. 9, no. 91, p. 569.
- 2) Nakanishi, K.; Nonoyama, F. *Toyota Technical Review*. 1995, vol. 30, no. 4, p. 35.
- 3) Kaiso, M. *The Special Steel*. 2010, vol. 59, no. 3, p. 18.
- 4) Hoshino, T.; Amano, K.; Tabata, N.; Nakano, S. *Kawasaki Steel Technical Report*. 1992, no. 26, p. 78.
- 5) Tashiro, H.; Sato, H. *Journal of the Japan Institute of Metals*. 1991, vol. 55, no. 10, p. 1078.
- 6) William C. Leslie. *The Physical Metallurgy of Steels*. Marzen Co., Ltd, 1985, p. 98.
- 7) Urita, T.; Namiki, K.; Iikubo, T. *Electric Furnace Steel*. 1988, vol. 59, no. 1, p. 33.
- 8) Kinoshita, S.; Ueda, T.; Suzuki, A. *Tetsu-to-Hagané*. 1973, vol. 59, no. 8, p. 58.
- 9) Murakami, T.; Hatano, H.; Yaguchi, H. *Kobe Steel Eng. Rep.* 2006, vol. 56 no. 3, p. 59.
- 10) Adachi, A.; Ogino, Y. *Jpn. Inst. Met.* 1966, vol. 30, no. 4, p. 394.
- 11) Kinoshita, S.; Ueda, T.; Suzuki, A. *J. Jpn. Inst. Met.* 1970, vol. 34, no. 8, p. 861.
- 12) Tsubota, H.; Takahashi, T.; Kobayashi, K. *Tetsu-to-Hagané*. 1981, vol. 67, no. 5, p. S562.
- 13) Narita, K.; Miyamoto, A. *Tetsu-to-Hagané*. 1964, vol. 50, no. 2, p. 174.
- 14) Ogino, Y.; Tanita, H.; Kitaura, M.; Adachi, A. *Tetsu-to-Hagané*. 1971, vol. 57, no. 3, p. 533.
- 15) Adachi, A.; Mizukawa, K. *Tetsu-to-Hagané*. 1962, vol. 48, no. 5, p. 683.
- 16) Hashimoto, K. *J. Jpn. Soc. Technol. Plast.* 2005, vol. 46, no. 531, p. 304.
- 17) Hashimoto, K.; Tanaka, T.; Nishimori, H.; Hiraoka, K. 2005 SAE International Congress & Exposition, SAE Technical Paper Series, p. 2005-01-0985.
- 18) Okamoto, N.; Shindo, Y.; Nagahama, M. *Kobe Steel Eng. Rep.* 2011, vol. 61, no. 1, p. 66.
- 19) Alogab, K. A.; Matlock, D. K.; Speer, J. G.; Kleebe, H. *J. ISIJ Int.* 2007, vol. 47, no. 7, p. 1034.
- 20) R. F. de Moraes; A. Reguly; L. H. de Almeida. *J. Mat. Eng. PERFORM.* 2006, vol. 15, p. 494.
- 21) Tanaka, T.; Hiraoka, K. *CAMP-ISIJ*. 2003, vol. 16, p. 1438.
- 22) Nagaoka, T.; Iguchi, M.; Kobayashi, K. *Sanyo technical report*. 1999, vol. 6, no. 1, p. 41.
- 23) Leap, M. J.; Brown, E. L. *Mater. Sci. Technol.* 2002, vol. 18, p. 945.
- 24) Cogne, J. Y.; Heritier, B.; Monnot, J. *Clean Steel*. 1987, vol. 3, p. 26.
- 25) Gladman, T. *Proc. Roy. Soc.* 1966, vol. 294, p. 298.
- 26) *J. Jpn. Soc. Technol. Plast.* 1981, vol. 22, p. 139.
- 27) Kazinczy, F.; Axnas, A.; Pachleiter, P. *Ann.* 1963, vol. 147, p. 788.
- 28) Smith, R. P. *Trans. AIME*. 1962, vol. 224, p. 190.
- 29) Narita, K.; Koyama, S. *Kobe Steel Eng. Report*. 1966, vol. 16, p. 179.
- 30) Meyer, L. Z. *Metallk.* 1967, vol. 58, p. 396.
- 31) Johansen, T. H.; Christensen, N.; Angland, B. *Trans. Met. Soc. AIME*. 1967, vol. 239, p. 1651.
- 32) Nordberg, H.; Aronsson, B. *JISI*. 1971, vol. 209, p. 1263.
- 33) Ohtani, H.; Hasebe, M.; Nishizawa, T. *CALPHAD*. 1989, vol. 13, p. 183.
- 34) Balasubraminian, K.; Kroupa, K.; Kirkaldy, J. S. *Metall. Trans.* 1992, vol. 23A, p. 729.
- 35) Hudd, R. C.; Jones, A.; Kale, M. N. *JISI*. 1971, vol. 209, p. 121.
- 36) Irvine, K. J.; Pickering, F. B.; Gladman, T. *JISI*. 1967, vol. 205, p. 161.
- 37) Ueno, M.; Itoh, K. *Tetsu-to-Hagané*. 1988, vol. 74, p. 1073.
- 38) Fukuoka, K.; Tomita, K.; Shiraga, T. *JFE Technical Report*. 2010, no. 15, p. 17.
- 39) Kurebayashi, Y. 188-189 Nishiyama Kinen Gijutsu Koza. 2006, p. 83.
- 40) Inoue, T.; Kinoshita, S. *Tetsu-to-Hagané*. 1976, vol. 62, no. 7, p. 875.